EUROFUSION WPJET1-PR(14) 12714

GMD Hogeweij et al.

Impact of W on scenario simulations for ITER

Preprint of Paper to be submitted for publication in Nuclear Fusion

This work has been carried out within the framework of the EUROfusion Consortium and has received funding from the Euratom research and training programme 2014-2018 under grant agreement No 633053. The views and opinions expressed herein do not necessarily reflect those of the European Commission.

Impact of W on scenario simulations for ITER

G.M.D.Hogeweij[1*], V. Leonov[2], J. Schweinzer[3], A.C.C. Sips[4], C. Angioni[3], G. Calabrò[5], R. Dux[3], A. Kallenbach[3], E. Lerche[6], C. Maggi[7], Th. Pütterich[3], ITPA Integrated Operating Scenarios topical group, ASDEX Upgrade team and JET Contributors †

EUROfusion Consortium, JET, Culham Science Centre, Abingdon, OX14 3DB, UK
[1] FOM-Institute DIFFER, Association EURATOM-FOM, P.O.Box 1207, Nieuwegein, The Netherlands, www.differ.nl
[2] IFT, NRC Kurchatov Institute, Moscow, Russia
[3] Max-Planck-Institut für Plasmaphysik, Garching, Germany
[4] European Commission, Brussels, B-1049, Belgium
[5] Associazione EURATOM-ENEA, Frascati, Italy
[6] Association EURATOM-Etat Belge, ERM-KMS, Brussels, Belgium
[7] EURATOM/CCFE Fusion Association, Culham Science Centre, Abingdon OX14 3DB, UK
∗E-mail: g.m.d.hogeweij@differ.nl

† *See the Appendix of F. Romanelli et al., Proceedings of the 25th IAEA Fusion Energy Conference 2014, Saint Petersburg, Russia*

Abstract. In preparation of ITER operation, large machines have replaced their wall and divertor material to W (ASDEX Upgrade) or a combination of Be for the wall and W for the divertor (JET). Operation in these machines has shown that the influx of W can have a significant impact on the discharge evolution, which has made modelling of this impact for ITER an urgent task. This paper reports on such modelling efforts. Maximum tolerable W concentrations have been determined for various scenarios, both for the current ramp-up and flat-top phase. Results of two independent methods are presented, based on the codes ZIMPUR plus ASTRA and CRONOS, respectively. Both methods have been tested and benchmarked against ITER-like I_p RU experiments at JET. It is found that W significantly disturbs the discharge evolution when the W concentration approaches $\sim 10^{-4}$; this critical level varies somewhat between scenarios.

PACS numbers: 52.25.Fi, 52.55.Fa, 52.50.Gj

Submitted to: Nucl. Fusion

1. Introduction - Summary of experimental results and ITER scenario Modelling

Recent experiments at ASDEX Upgrade (W limiter and divertor) and JET (W divertor) showed that core W accumulation can have several detrimental effects: a (periodic) loss of the H-mode, as observed in ASDEX Upgrade [1]; strongly perturbed T_e and q profiles during the I_p Ramp Up (RU), as observed in JET [2]; a hollow T_e profile during H-mode, leading to locked MHD modes and finally a disruption in JET [3]. Figure 1 shows examples of W accumulation in JET and ASDEX Upgrade.

The W level in the ITER core plasma will be determined by many factors. The first factor is the influx through the separatrix, which will depend on the source (divertor sputtering) and which is strongly influenced by the state of the plasma in the Scrape Off Layer (SOL), which can vary from attached to fully detached [4]. The second factor is the transport through the Edge Transport Barrier (ETB), where the relative steepness of electron density (n_e) and ion temperature (T_i) in the ETB can both result in peaked and hollow W profiles [5], and where ELMs can flush W. The third factor is core diffusive and convective W transport. Comparison between theory and experimental data has shown that, at least in the inner core, neoclassical transport is the dominating contributor to core W transport [6, 7, 8]. This knowledge, which implies strong dependence of the n_W profile on the relative steepness of the n_e and $T_i$profiles, will be used in part of the modelling work discussed in this paper. The fourth factor is core MHD; e.g. periodic sawteeth can flush W from the core. For these reasons even a complete and perfect transport model could only predict core W concentrations after several assumptions have been made.

Predictions for ITER operating scenarios have been developed for many years [9, 10, 11, 12, 13]. Good progress has been made recently in incorporating particle transport models in scenario simulations for the ITER baseline which has the goal of reaching energy gain $Q = 10$ with ~ 500 MW of fusion [14, 15].

This contribution reports on the impact of including W in the simulations for ITER scenarios, based on the interpretation and extrapolation of results obtained for stable H-mode operation in ASDEX Upgrade and JET [1, 16] and from ITER-like plasma current (I_p) ramp-up (RU) and ramp-down (RD) experiments at JET [2]. The work concentrated on assessing the W content of the core of ITER plasma and the effect of the radiation by W on plasma performance and the evolution of the discharge. Hence for various ITER scenarios the level of W concentration has been determined above which the ITER plasma leaves the allowed or desired operational space, in terms of e.g. l_i, q profile, flux consumption. and energy gain Q. This level will be called the *critical level*. Flux consumption in this paper is always referring the total flux consumption, i.e. the sum of the resistive and inductive contribution.

Because of the many uncertainties affecting core W concentration in ITER, as sketched above, it is attractive to take a pragmatic view. Hence, in stead of carefully modelling W transport from divertor source through SOL, separatrix, ETB into the core,

in this paper certain W concentrations have been assumed as given and their effect on the discharge evolution was calculated. This was done in two ways: *(i)* either a given W concentration is assumed for the whole core plasma, *(ii)* or only the W concentration at the separatrix was assumed, in which case simplified transport models were used to predict the core W concentration. The only exception to this will be in section 4.1 on the limiter phase of the I_p RU, where the impurity source (limiter sputtering) is taken into account.

In the realization of ITER scenarios the superconducting poloidal field (PF) coil system plays a crucial role. First, it must provide a stable plasma equilibrium; second, it must be able to provide the significant amount of magnetic flux that is needed to ramp up the plasma current inductively, and then keep the current flattop phase for a sufficiently long time. The ITER PF coils must remain within several limits, such as coil current, coil field, voltage, power and central solenoid force limits. Allowing for control margins, the PF system of ITER will only allow a range of $l_i = 0.7 - 1.0$ [17] (note that throughout this paper l_i refers to $l_i(3)$, as defined in e.g. [17]). Therefore, in the judgement whether a certain W concentration is acceptable, the primary criteria are the value of l_i and the flux consumption.

It is important to include in the predictions for ITER the key observations of the experiments. However, assuming ITER will reach the temperatures expected, basic radiation calculations for high-Z impurities indicate that ITER will be in a different situation from present-day machines; the W radiation is concentrated in the outer half of the plasma, while W radiates in the core at ASDEX Upgrade and JET. Hence results of present-day machines can not be extrapolated to ITER directly.

The work presented here on scenario simulations for ITER, including the effect of W on the discharge evolution, have been initiated by the Integrated Operation Scenarios Topical Group (IOS-TG) of the ITPA. Within the IOS-TG various simulation methods were applied to achieve this goal. In the present work two methods will be presented and compared, one based on the combination of ZIMPUR and ASTRA, and one based on CRONOS.

The paper is organized as follows. Section 2 gives details on the transport codes and models used for the simulations. W accumulation observations in the JET-ILW I_p RU phase have been used to test and benchmark the modelling, which is reported in Section 3. The main part of the paper is then the ITER modelling, as reported in Sections 4 and 5. Finally, in section 6 consequences for future ITER operation are discussed.

2. Modelling codes and choices

For the JET simulations n_e profiles, Z_{eff} evolution, and boundary conditions for $T_{e,i}$ and n_e were taken from experimental data. For ITER, these input data were adopted from the ITER team.

All modelling presented is essentially 1D, i.e. poloidal asymmetries are not taken into account. Even in the relatively slow rotating ITER plasma, with a Mach number

of the main plasma of e.g. $M_{\mathrm{D,T}} \sim 0.1$, for W one would have $M_{\mathrm{W}} \sim 1$. So centrifugal effects are not expected to be negligible in ITER. However, moving away from the Pfirsch-Schlüter regime towards lower collisionality regimes for impurities, the impact of centrifugal effects on the neoclassical convection to diffusion ratio is reduced [8, 18].

2.1. ZIMPUR + ASTRA

The first tool used is the combination of the ZIMPUR code [19] for the modelling of impurity behaviour (including neoclassical and anomalous transport for impurities and non-coronal radiation), with ASTRA [20] for the evolution of the bulk plasma parameters.

In ASTRA a scaling based transport model was used. The standard set of transport equations for T_{i}, T_{e}, n_{d} was solved assuming

$$\chi_{\mathrm{e}} = D_{\mathrm{d}} = D_{\mathrm{an}} = D_0 \cdot F(\rho) F_{\mathrm{H}} \qquad \chi_{\mathrm{i}} = 2 D_{\mathrm{an}} \tag{1}$$

where $F_{\mathrm{H}} = 1$ except for the edge barrier region, and the radial profile of transport coefficients was taken of the form:

$$F(\rho) = 1 + 3\rho^2 \quad \text{with} \quad \rho_N = \rho / \rho_{max} \tag{2}$$

The normalization coefficient D_0 was adjusted to provide tau_{E} as given by the ITER L- or H-mode scalings in the ITER case, or the best possible match of simulated and experimental radial profiles in the JET case. Convective terms were taken into account in the heat transport equations in the form of $3/2 \cdot T \cdot \Gamma$. For the H-mode cases the external transport barrier region ($\rho_N > 0.93$) was simulated by reducing the factor F_{H} for this region such that

$$\chi_{\mathrm{e}} = \chi_{\mathrm{i}} \simeq {\chi_{\mathrm{i}}}^{\mathrm{nc}} \tag{3}$$

in order to reproduce pedestal profiles.

The transport coefficients used for the different impurity ions are the sum of the anomalous (D_{an}) and neoclassical (NC) contributions. For the latter the total matrix of the NC coefficients for all different ions is used, taking into account collisions between all ions. Production and penetration of W is treated as a 1D process.

2.2. CRONOS

The second tool used is the CRONOS suite of codes [21]. Self-consistent simulations of the I_{p} RU phase were performed both for JET-ILW ITER-like pulses, and for ITER hybrid scenario pulses. Evolution of T_{e}, T_{i} and j were modelled self-consistently.

The semi-empirical Bohm-gyroBohm transport model was used (L-mode version, [22]). In the past this model has proven to give good reproductions of the I_{p} RU phase in JET [23]. See [24] for details. It should be noted that theoretical models like GLF23 do not reproduce well the ohmic and L-mode I_{p} RU [23]. Sawteeth were taken into account in the modelling; the Porcelli model was used to describe the sawtooth crash

[25]. The radiation was calculated, using detailed atomic physics [26]; the predictions of this model only slightly deviate from the simple average ion model [27].

3. Modelling of the I_p RU phase of JET

3.1. ZIMPUR + ASTRA

To benchmark the radiation calculation in ZIMPUR, a JET case with strong W accumulation during the I_p RU was modelled predictively (JPN 83444), i.e. the evolution of T_e, T_i (ASTRA), n_W and P_{rad} (ZIMPUR) were simulated, including the external heat sources (5.1 MW of NBI in this case). The inward neo-classical W convection was not strong enough to reproduce the extreme W peaking in this case; therefore the inward convection was artificially enhanced for $\rho < 0.3$. It should be noted, however, that this modelling neglects the impact of centrifugal effects, which are certainly not negligible for JPN 83444; one of the main effects of rotation is reducing the impact of temperature screening, and therefore increasing the inward component of the neoclassical convection [28]. In these simulations the W flux at the boundary was not calculated, but simply chosen to reproduce the correct n_W in the core.

Results are summarized in Fig.2. It can be seen that ZIMPUR reproduces quite well the measured P_{rad} profile, and that ASTRA correctly predicts the observed hollow T_e profile.

3.2. CRONOS

To prepare scenarios for ITER, the discharge evolution during the ITER-like current ramp-up phase in JET was modelled with the CRONOS suite of codes for different W concentrations. In some of these pulses strong W accumulation was observed [29]. The experimental data (T_e, n_e, Z_{eff}) were used. n_W/n_e profiles were assumed either flat or using the same (peaked) shape as measured in the experiments.

Using the experiments as a basis, the W concentration was scanned for the simulations of the current ramp up in JET. A critical W concentration of $\simeq 10^{-4}$ was calculated for a current ramp-up in H-mode at JET. Also the impact of the shape of the W profile in the plasma was studied. With a flat n_W/n_e (representing cases where the W peaking is controlled), the effect of high W concentration is a global decrease of T_e leading to increased flux consumption, without strong change of the q profile. With a peaked n_W/n_e (core impurity accumulation), above the critical n_W/n_e a hollow T_e profile and reversed shear develop, without strong change of plasma inductance (l_i) or flux consumption. These results are in excellent agreement with experimental findings; for details the reader is referred to [2]. Similar modelling for ASDEX Upgrade is in progress.

4. Modelling of ITER I_p ramp up and flat top phase with ZIMPUR

4.1. Limiter phase of the I_p RU

Fig.3 shows the calculated evolution of discharge parameters during I_p RU stage of the inductive ITER scenario at $I_p < 7.5$ MA for the limiter phase of the discharge, i.e. before X-point formation. Note that in this simulations a W limiter was assumed. In the simulations the plasma column was formed initially near the limiter, which fixed plasma size. Then simultaneously with the I_p rise, the plasma column was shifted to the vacuum vessel center. In this stage bombardment of the limiter by ions accelerated in the limiter sheath potential results in the limiter surface erosion. Limiter sputtering by bulk D/T ions escaping the plasma and self-sputtering by ions of limiter material with different charge on the plasma periphery are the main sources of impurities in the plasma. To estimate the maximum effect, sheath potential reduction due to the secondary electron emission and reduction of the edge plasma temperature due to increase of the particle recycling on the limiter have not been taken into account. Prompt redeposition of W is not taken into account. Recent studies [30] indicate that this prompt redeposition is expected to be very high, so the calculated source is a pessimistic upper limit.

Simulations show that in the early low density I_p RU phase W contamination increases to $\sim 0.05\%$ of n_e and then decreases together with the rise of n_e. The most critical was the phase up to 4-5 s when P_{rad} is near the total power injected into the plasma. On the one hand, radiation of power helps to stabilize boundary temperature on a relatively low level of $\sim 40-50$ eV when limiter sputtering is small (negative feedback). On the other hand, it can impede current rise and at some higher W contamination there is a danger of radiative collapse.

4.2. Flat top

Values of critical impurity concentrations are defined by the available level of auxiliary heating power and accessible Q values. At higher impurity concentration either the fusion gain factor (Q) drops below the desired value of 5, or the power flux through the separatrix drops below the H-L-mode threshold power, thus inducing transition to L-mode with deterioration of confinement and further plasma cooling. Fig.4 demonstrates the dependence of plasma parameters on impurity concentrations for the flat-top stage of the reference inductive ITER scenario. The critical concentrations of different impurities expected for this scenario are found in this figure at $P_{aux} \leq 73$ MW and $Q \geq 5$. Table 1 summarizes estimations for other reference ITER scenarios. For example the calculated critical W concentration (n_W/n_e) is about $7 \cdot 10^{-5}$ for the inductive scenario and a factor of 2-3 lower for the hybrid and steady-state scenarios.

5. Modelling of the impact of W on the I_p RU phase of ITER with CRONOS

Self-consistent simulations of the I_p RU phase for the ITER hybrid scenario were performed with the CRONOS suite of codes. Three different assumptions on the W concentration profile have been used: flat, peaked, and determined by neoclassical transport; each of them will be discussed in the following.

5.1. Assuming flat n_W/n_e profile

In a first series of simulations, a fixed n_W/n_e concentration was assumed, with a flat radial profile. Additional power can balance the increased radiation at high W concentration, thus increases the maximum tolerable W level. The main cooling effect of W with a flat radial n_W/n_e profile is off-axis, leading to increasingly peaked T_e profiles; therefore the additional power was chosen to be off-axis with $\rho_{dep} = 0.5$. Hence both ohmic and L-mode plasmas were simulated; the latter had, starting at 30 s, 20 MW of off-axis ECRH with $\rho_{dep} = 0.5$. For cases with high n_W, also high power L-mode was considered, where in addition to the 20 MW of off-axis ECRH also 20 MW of on-axis ICRF was applied. As seen in Fig.5, for an ohmic ITER ramp-up a flat n_W/n_e profile with $n_W/n_e \geq 1 \cdot 10^{-4}$ leads to unacceptably high l_i. For $n_W/n_e \geq 2 \cdot 10^{-4}$ the simulated plasma is choked at a certain moment because P_{rad} exceeds P_{ohm}. However, using 20 MW of ECRH from early in the ramp-up, the critical level would be increased by a factor of $\simeq 2$; still the plasma is choked for $n_W/n_e \geq 5 \cdot 10^{-4}$ when at a certain time P_{rad} exceeds $P_{ohm} + P_{ECH}$. Adding additional 20 MW of ICRF further enhances these limits by a factor of ~ 2.

5.2. Assuming peaked n_W/n_e profile

In a second series of simulations, a peaked n_W/n_e concentration was assumed. Again both ohmic and L-mode plasmas were simulated; the latter had 10 MW of nearly central ECRH and in one cases additionally 20 MW of central ICRF. In the simulations a peaking of a factor 5-10 was assumed inside $\rho = 0.15 - 0.3$. Simulations with peaked n_W/n_e do not obtain the high $l_i$values seen in the simulations using flat n_W/n_e. However, too high central n_W/n_e ($\simeq 2 \cdot 10^{-4}$ in the ohmic case, $\simeq 10^{-3}$ in the L-mode case) causes a net sink in the centre, leading to hollow T_e profiles and perturbed q profiles, and finally the plasma is choked; see Fig.6.

5.3. Assuming neo-classical core W transport

Finally, in order to have more realistic predictions, a simple W transport model was adopted. There are strong indications that, at least in the inner core, neoclassical transport is the dominating contributor to W transport [6, 7, 8]. If it were the only

contributor, one would expect following relation between inverse gradient lengths [31]:

$$1/L_{\mathrm{n}_{\mathrm{Z}}^{\mathrm{neocl}}} = Z(1/L_{\mathrm{n_i}} - 1/2 \cdot 1/L_{\mathrm{T_i}}) \tag{4}$$

We will take $Z = 40$, which is correct for W in the core of JET and ASDEX Upgrade (few keV). For the ITER core (20 keV) $Z = 60$ would be more realistic [26]; however, this will hardly have an effect on the simulation results. It should be noted that Eq.4 is only correct in steady state; n_{W} will react to changes in n_{e} and T_{i} on a time scale of approximately ${L_{\mathrm{n}}}^2/D_{\mathrm{neo}}$. In the simulations so far this effect has been neglected. Assuming that the turbulence mechanisms governing particle transport are the same for all species, it is sensible to assume

$${n_{\mathrm{W}}}^{turb} \sim n_{\mathrm{e}} \tag{5}$$

Due to the high Z value, Eq.4 could yield extremely hollow or peaked n_{W} in the inner core. Residual turbulent transport and MHD will make these profiles less extreme; hence we assume in the inner core n_{W} to be a combination of ${n_{\mathrm{W}}}^{nc}$ and ${n_{\mathrm{W}}}^{turb}$, which leads to:

$$\begin{aligned} &\text{for } \rho \geq \rho_{bd} : n_{\mathrm{W}} = {n_{\mathrm{W}}}^{turb} = \gamma \cdot n_{\mathrm{e}} \\ &\text{for } \rho \leq \rho_{bd} : n_{\mathrm{W}} = \zeta\gamma \cdot n_{\mathrm{e}} + {n_{\mathrm{W}}}^{nc} \\ &\text{where } {n_{\mathrm{W}}}^{nc}(\rho_{bd}) = (1-\zeta)\gamma \cdot n_{\mathrm{e}}(\rho_{bd}) \end{aligned} \tag{6}$$

where ${n_{\mathrm{W}}}^{nc}$ obeys Eq.4, and the match of the first two formulas of Eq.6 at ρ_{bd} yields the last formula. In the simulations we take

$$\gamma = 10^{-4} \qquad \zeta = 0.5 \qquad \rho_{bd} = 0.4 \tag{7}$$

The crucial point is the peakedness of the n_{e} profile. We will assume three concave parabolic shapes with low, medium, high and very high peaking factor $n_{\mathrm{e}}(0)/\langle n_{\mathrm{e}} \rangle = 1.3, 1.47, 1.57$ and 1.66, respectively. The latter may seem unrealistically high; however, it should be noted that scaling studies predict a peaking factor of $\simeq 1.5$ for ITER, due to its low collisionality [32, 33].

Simulation results are summarized in Fig.7, both for cases with constant n_{e} peaking and for cases with low initial n_{e} peaking and higher n_{e} peaking in the later ramp-up phase. If no additional heating is applied during the I_{p} RU, then

- The case with low density peaking yields, due to temperature screening, a hollow n_{W} profile.
- In the intermediate case, n_{W} is well controlled during the ramp-up; however, soon after the I_{p} RU the plasma is choked due to a sudden W peaking.
- In the peaked case the plasma is choked already after 9 s due to extreme W peaking.
- When the density becomes peaked halfway the I_{p} RU, the plasma survives for at least 30 s before strong W peaking sets in.

In all cases, additional 10 MW centrally deposited ECRH is sufficient to keep the plasma parameters within the allowed limits. Central electron heating increases, due to the strong electron-ion coupling, also T_i peaking, hence increases temperature screening. A second beneficial effect of central ECRH, not taken into account here, would be increased turbulent W transport. If n_e becomes suddenly more peaked during the I_p RU, then there is sufficient time left to switch on ECRH: in the simulations ECRH was switched on 10 s after the n_e peaking started, and this was sufficient to keep the plasma parameters within the allowed limits.

5.4. Other points of concern

So far this section was only concerned about the effect of W accumulation during the I_p RU on crucial parameters like l_i and the risk of choking the plasma when $P_\mathrm{rad} > P_\mathrm{in}$. First, it should be realized that these limits are important during the whole duration of the discharge; in particular, the effect of W on the exit of the burn phase and current ramp down requires further study. Second, there are other critical parameters to be observed. Two of them, the radiation at the time of entry to H-mode and the flux consumption are assessed in this subsection.

5.4.1. L-H transition The available auxiliary power in ITER (ECRH, ICRF, NBI) is expected to be only marginally above the L-H threshold power (P_LHthr), which is expected to be near 50 MW [34]. As the critical parameter for the L-H transition is the heat flux through the separatrix, a significant amount of core radiation would mean that P_LHthr can not be attained. Fig.8 shows, both for ohmic and L-mode I_p RU, P_rad as function of line averaged $n_\mathrm{W}(0)/n_\mathrm{e}(0)$ for the case of flat (left) and peaked (right) $n_\mathrm{W}/n_\mathrm{e}$ profiles at 60 s, i.e. at 3/4 of the I_p RU. In the latter case $n_\mathrm{W}/n_\mathrm{e}$ is inside $\rho = 0.25$ assumed to be a factor of 10 larger than outside. As can be seen, P_rad rises more or less linearly with $n_\mathrm{W}/n_\mathrm{e}$, and for $n_\mathrm{W}/n_\mathrm{e} \simeq 2 \cdot 10^{-4}$ one has $P_\mathrm{rad} \simeq 10$ MW, which can be considered as a significant fraction of P_LHthr.

5.4.2. Flux consumption Also the increased flux consumption due to W accumulation is a point of concern. The inductive flux will not change much; hence only the resistive flux consumption will be considered. Fig.9 shows the resistive flux consumption up to 60 s as function of $\langle n_\mathrm{W}/n_\mathrm{e} \rangle$, for various heating schemes. For a given heating scheme a W concentration if $2 \cdot 10^{-4}$ causes an increase of flux consumption by 20-30 Vs. Given the typical loop voltage in the flat-top of 0.02-0.04 V, this would mean that the projected flux consumption of the whole flat-top would already be consumed in the I_p RU phase. On the other hand, the red points in the plots from cases with extremely early switch-on of strong auxiliary heating (30-40 MW of ECRH plus ICRF from 10 s) show that such a heating scheme would reduce flux consumption to the normal level (i.e. without W accumulation).

5.5. Summary

The critical W concentrations during I_p RU are summarized in Table 2, both for the assumption of flat and peaked n_W/n_e. The numbers are approximations, since no fine scan of n_W/n_e was performed. In the case of flat n_W/n_e the critical concentration is reached when l_i exceeds the allowed maximum value for ITER of 1. In the case of peaked n_W/n_e hollow T_e profiles may develop. However, when this happens then usually the plasma is choked later on; therefore this was not added in the table as a separate critical value.

6. Discussion, Conclusion and Outlook

Critical W concentrations have been determined, both for the I_p RU phase and for the flat-top phase of various ITER scenarios, using two different suites of codes: first ZIMPUR plus ASTRA, second CRONOS. Both were successfully tested against experimental JET data. The results of the different codes are consistent. The main results are summarized in Tables 1 and 2.

For the ohmic I_p RU phase, the critical W concentration is a few times 10^{-5}; with 10-20 MW of additional heating this limit is enhanced by a factor of $\simeq 2$. For maintaining $Q > 5$ at 15 MA in ITER the W concentration should be below $7 \cdot 10^{-5}$.

Apart from assuming certain n_W concentrations (flat or peaked), also the assumption of the n_W profile being fully determined by neo-classical transport was exploited. the latter assumption leads to an extreme sensitivity of the n_W profile on the peaking of the n_e and T_i profiles. This sensitivity was also found for simulations of n_W profiles in the ETB, which may vary from very peaked to very hollow [5].

As critical W concentrations have now been calculated for different ITER scenarios, future work can concentrate on further quantification of these limitations. For this purpose the maturing understanding of neoclassical and anomalous W transport can be used. One important aspect missing in the modelling presented in this paper is the centrifugal effect. The main effect of centrifugal forces at ITER core parameters can be expected to be an increase of the neoclassical diffusivity (as compared to non-rotation calculations). This can be significant also at small rotation values, since the effect increases strongly with Mach number. This will impact the relative weight of neoclassical and turbulent transport components [8, 18]. In the simplified model of section 5.3 this would impact the location of ρ_{bd} and the magnitude of coefficient ζ in Eq.6, which would in principle allow a parameterization of centrifugal effects in the modelling of Section 5.3.

Another aspect to be improved in future work is the choice of the core transport model. Both models used in this paper, a scaling based model in Section 4 and the Bohm-gyroBohm model in Section 5, are (semi-)empirical. A theoretical model which has been proven successful for the I_p RU phase of ASDEX-U is TGLF, when combined with a nonlinear enhancement of transport at the edge, motivated by theoretical arguments

and comparisons between nonlinear and quasi-linear simulations [35].

References

[1] Neu R. *et al IEEE Tr. Plasma Science* **42** (2014) 552
[2] Hogeweij G.M.D. *et al Nucl. Fusion* **55** (2015) 013009
[3] De Vries P.C. *et al Phys. Plasmas* **21** (2014) 056101
[4] Van Rooij G.J. *et al J. Nucl. Mat.* **438** (2013) S42
[5] Dux R. *et al Plasma Phys. Control. Fusion* **56** (2014) 124003
[6] Angioni C. *et al* 40th EPS Conf. on Plasma Physics (2013) P4.142
[7] Angioni C. *et al Nucl. Fusion* **54** (2014) 083028
[8] Casson F.J. *et al Plasma Phys. Control. Fusion* **57** (2015) 014031
[9] Kessel C.E. *et al* 2007 *Nucl. Fusion* **47** 1274
[10] Parail V. *et al* 2009 *Nucl. Fusion* **49** 075030
[11] Budny R.V. *et al* 2009 *Nucl. Fusion* **49** 085008
[12] Citrin J. *et al* 2010 *Nucl. Fusion* **50** 115007
[13] Kritz A.H. *et al* 2011 *Nucl. Fusion* **51** 123009
[14] Zagórski R. *et al* 2011 *J. Nucl. Mat.* **415** S483
[15] Ivanova-Stanik I. *et al* 2014 *Contr. Plasma Phys.* **54** 341
[16] Beurskens M.N.A. *et al Plasma Phys. Control. Fusion* **55** (2013) 124043
[17] A.C.C. Sips *et al* 2009 *Nucl. Fusion* **49** 085015
[18] Angioni C. *et al submitted to* Phys. Plasmas *2014*
[19] Leonov V.M., Zhogolev V.E., *Plasma Phys. Control. Fusion* **47** (2005) 903
[20] Pereverzev G.V. *et al ASTRA: Automated System for Transport Analysis in a Tokamak*, Max-Planck Institute Report, IPP 5/98
[21] Artaud J.-F. *et al Nucl. Fusion* **50** (2010) 043001
[22] Erba M. *et al Nucl. Fusion* **38** (1998) 1013
[23] Imbeaux F. *et al Nucl. Fusion* **51** (2011) 083026
[24] Hogeweij G.M.D. *et al Nucl. Fusion* **53** (2013) 013008
[25] Porcelli F. *et al* 1996 *Plasma Phys. Control. Fusion* **38** 2163
[26] Th. Pütterich *et al* 2010 *Nucl. Fusion* **50** 025012
[27] D. Post. *et al* At. Data Nucl. Data Tables 1977 **20** 397
[28] Angioni C. *et al Plasma Phys. Control. Fusion* **56** (2014) 124001
[29] G. Calabrò *et al* 40th EPS Conf. on Plasma Physics (Espoo, Finland) 2013, O2.106
[30] Chankin A.V. *et al Plasma Phys. Control. Fusion* **56** (2014) 025003
[31] Helander P., Sigmar D.J., *Collisional Transport in Magnetized Plasmas*, 2002, Cambridge University Press
[32] Weisen H. *et al Nucl. Fusion* **45** (2005) L1
[33] Angioni C. *et al Nucl. Fusion* **47** (2007) 1326
[34] Doyle E.J. *et al Nucl. Fusion* **47** (2007) S18
[35] Fable E. *et al Nucl. Fusion* **52** (2012) 063017

Acknowledgements

This work has been carried out within the framework of the EUROfusion Consortium and has received funding from the European Union's Horizon 2020 research and innovation programme under grant agreement number 633053. The views and opinions expressed herein do not necessarily reflect those of the European Commission This work is supported by NWO-RFBR Centre-of-Excellence on Fusion Physics and Technology (Grant nr. 047.018.002).

Table 1. *Critical relative concentrations of different impurities for the reference ITER scenarios*

	W	Ar	Be
Inductive	$\sim 7 \cdot 10^{-5}$	$\sim 2.5 \cdot 10^{-3}$	$\sim 5 \cdot 10^{-2}$
Hybrid	$(2-3) \cdot 10^{-5}$	$(1.2-2) \cdot 10^{-3}$	$(3-4) \cdot 10^{-2}$
Steady State	$(3-3.5) \cdot 10^{-5}$	$(1.8-2.2) \cdot 10^{-3}$	$(8-9.5) \cdot 10^{-2}$

Table 2. *Critical relative W concentration during ITER I_p RUin units of 10^{-4}. For the peaked case the value of n_W/n_e at the edge is given; inside $\rho = 0.25$ a 10 times higher concentration is assumed. Low power L-mode has 20/10 MW of ECRH in the flat/peaked case; high power L-mode has additionally 20 MW of ICRF.*

	Assuming flat n_W/n_e		Assuming peaked n_W/n_e
criterium	$l_i > 1$	plasma choked	plasma choked
ohmic	1	2	0.5
low power L-mode	2	4	1
high power L-mode	5	8	

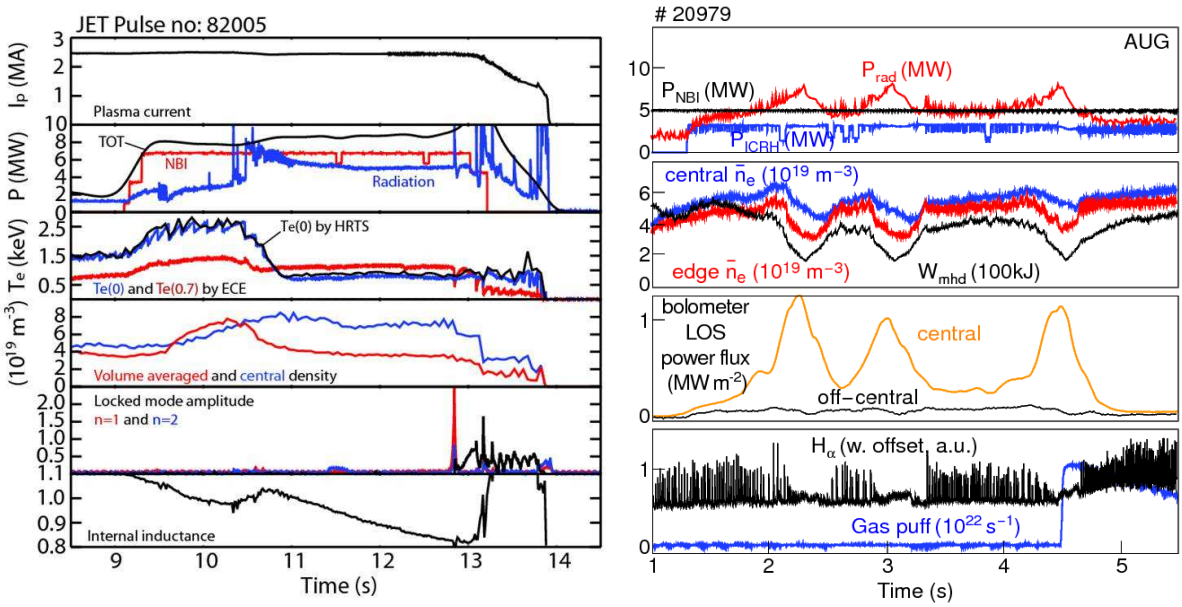

Figure 1. *Examples of W accumulation in JET leading to a hollow T_e profile, locked MHD modes and finally a disruption (left), and in ASDEX Upgrade (right caused a periodic loss of the H-mode (right). Figures taken from [3, 1].*

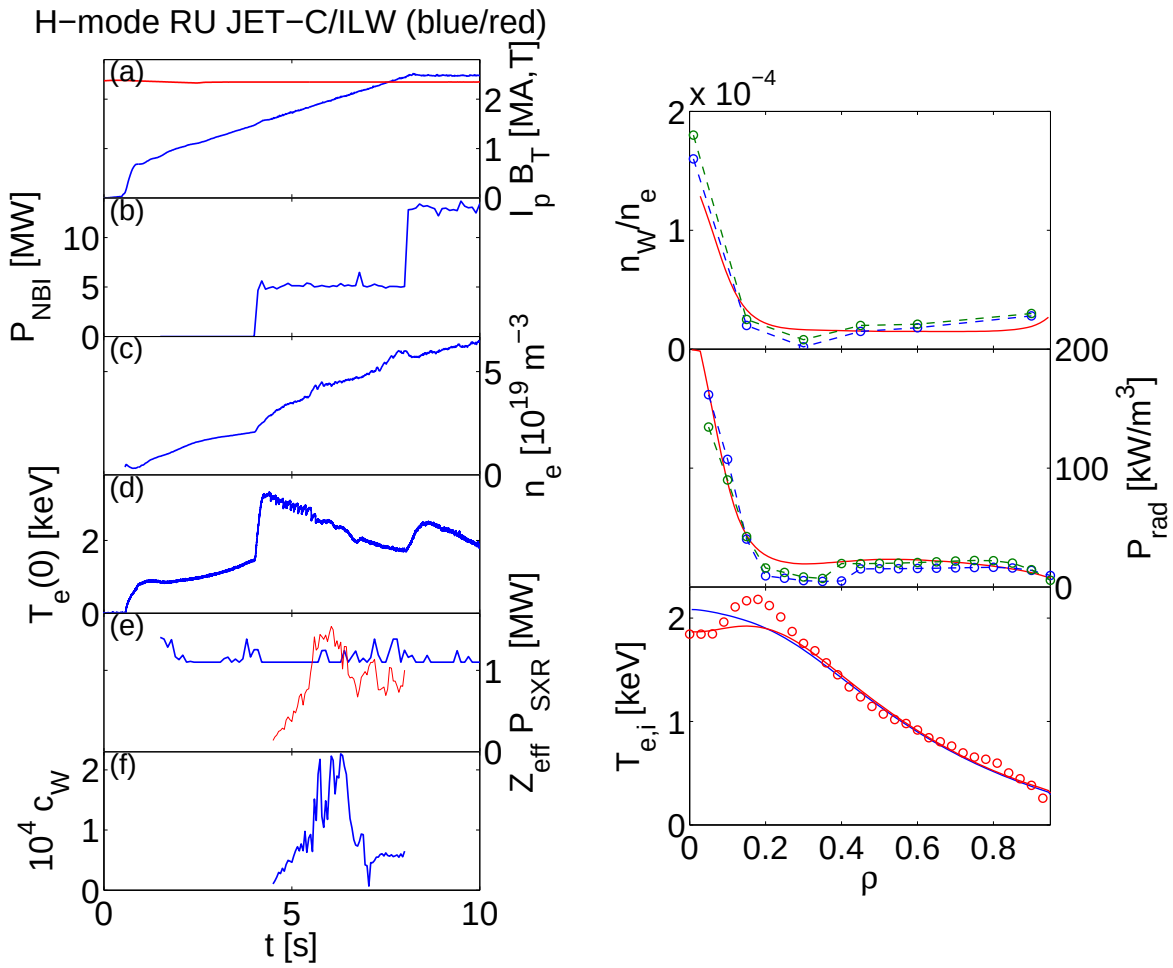

Figure 2. *Left: Experimental time traces of JPN 83444. Shown are* $I_{\rm p}$ *(blue) and* $B_{\rm t}$ *(red);* $P_{\rm NBI}$*; line averaged* $n_{\rm e}$*;* $T_{\rm e}(0)$*;* $Z_{\rm eff}$ *(blue) and total SXR radiation inside the separatrix (red); W concentration. The latter two signals are only available in the time window [4 8] s; before 4 s the low level of the SXR signal impedes the derivation of the W concentration. Right: Profiles of relative W density, radiated power density,* $T_{\rm e}$ *(red) and* $T_{\rm i}$ *(blue), as calculated by ZIMPUR+ASTRA, for JPN 83444 at 6s. Full lines: simulation; dashed lines and open circles: experimental data.*

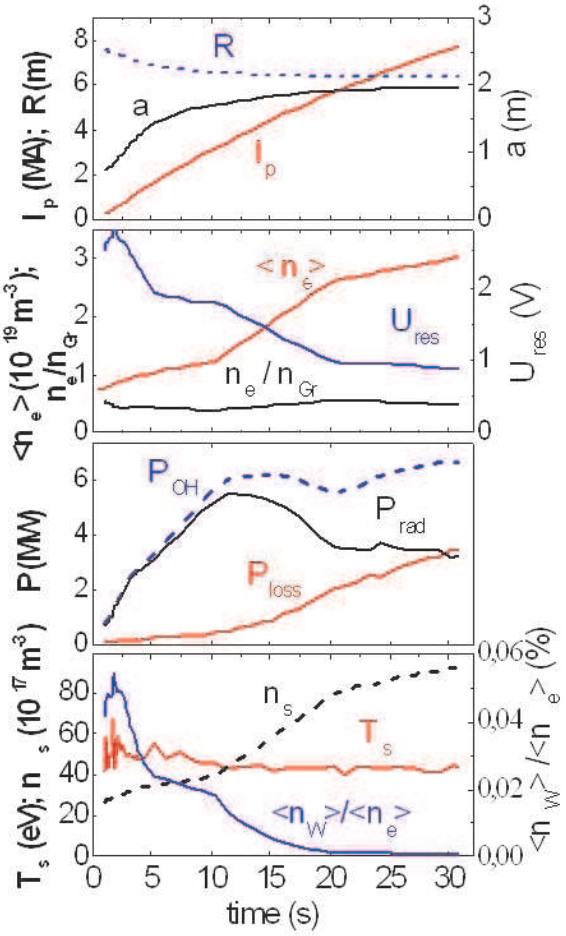

Figure 3. *Evolution of parameters during plasma current ramp-up stage of the inductive ITER scenario with tungsten limiter.*

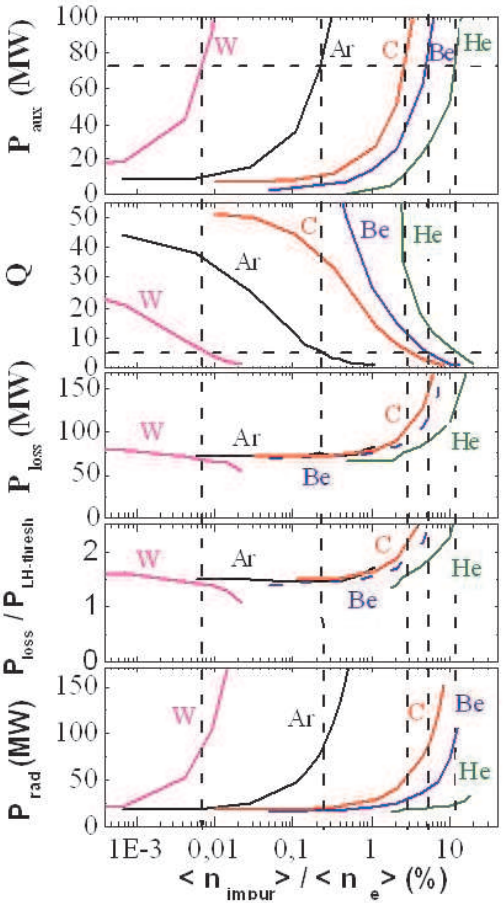

Figure 4. *Change of plasma parameters versus impurities concentrations.*

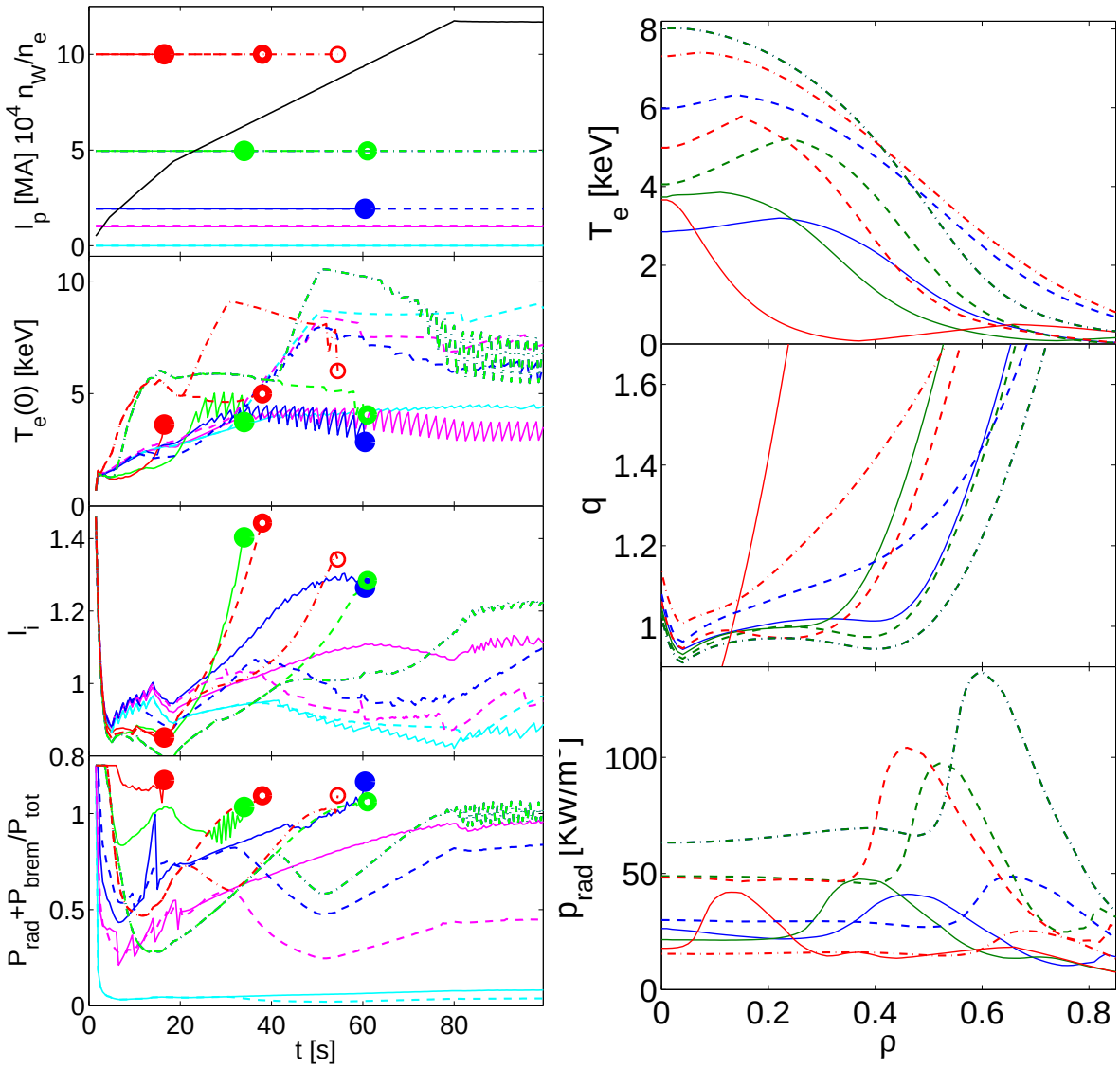

Figure 5. *Results of predictive modelling of various W concentrations, assuming flat* $n_{\mathrm{W}}/n_{\mathrm{e}}$*. Shown are ohmic (full lines) and L-mode cases (dashed lines: 20 MW of off-axis ECRH only; dashed-dotted lines: same ECRH plus 20 MW on-axis ICRF). Left panel: time traces of* $n_{\mathrm{W}}/n_{\mathrm{e}}$*,* $T_{\mathrm{e}}(0)$*,* l_{i}*, and* $P_{\mathrm{rad}}/P_{\mathrm{in}}$*. In some cases the simulated plasma is choked when* P_{rad} *exceeds* P_{in}*; these points are marked with a circle (filled: ohmic; semi-open: L-mode ECRH; open: L-mode ECRH+ICRF). Right panel: profiles of* T_{e}*,* q *and* P_{rad} *at the end of the* I_{p} *RU (80 s), with the same colour coding. For clarity the two cases with the lowest W concentration were omitted. In those cases when the plasma is choked, the profiles are taken just before the end of the simulation.*

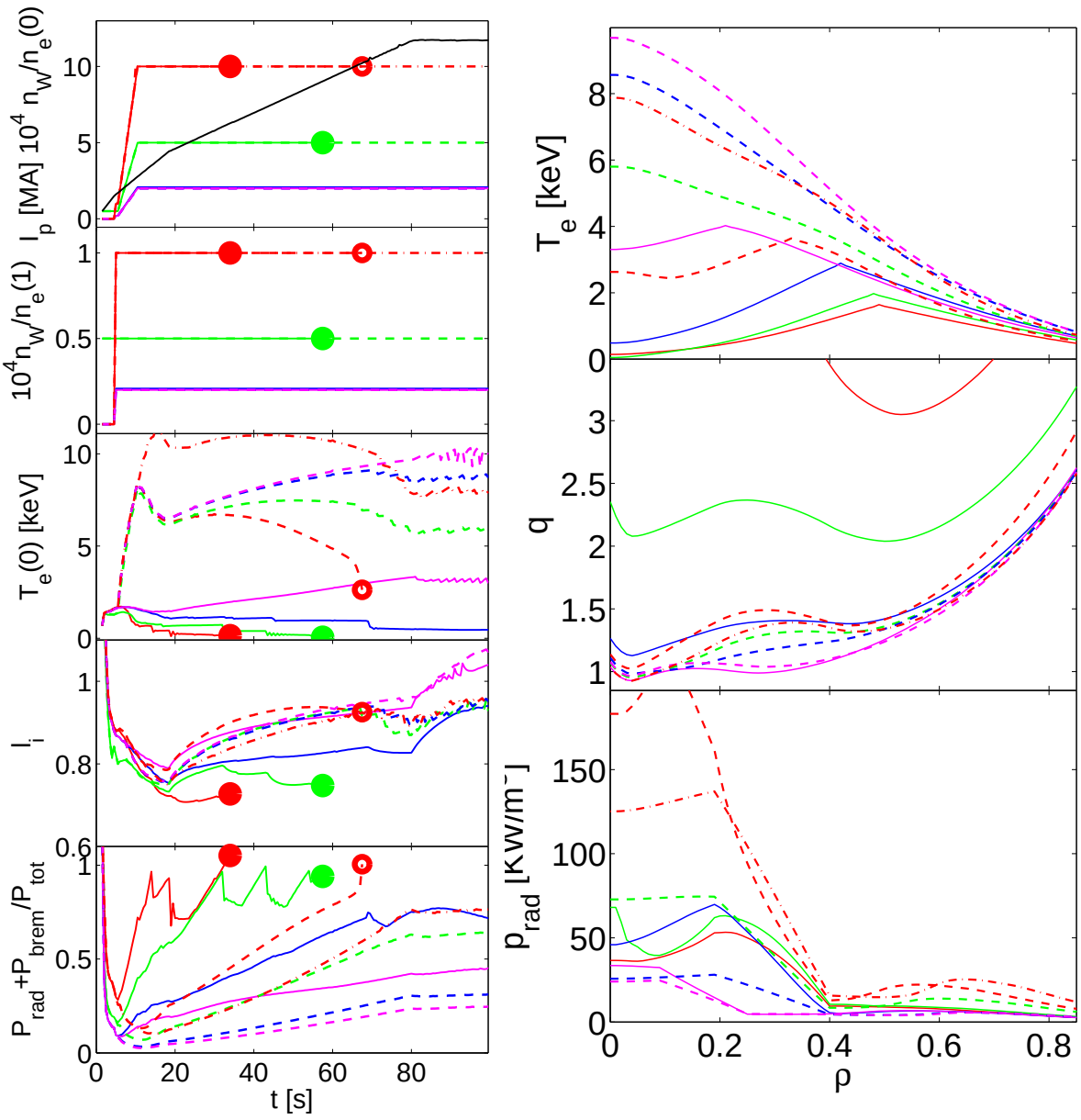

Figure 6. *Results of predictive modelling of various W concentrations, assuming peaked* $n_{\rm W}/n_{\rm e}$*. Shown are ohmic (full lines) and L-mode cases (dashed and dashed-dotted lines, see previous figure). Left panel: time traces of* $I_{\rm p}$*,* $n_{\rm W}(0)/n_{\rm e}(0)$*,* $n_{\rm W}(1)/n_{\rm e}(1)$*,* $T_{\rm e}(0)$*,* $l_{\rm i}$ *and* $P_{\rm rad}$*. Right panel: profiles of* $T_{\rm e}$*,* q *and* $P_{\rm rad}$ *at the end of the* $I_{\rm p}$ *RU (80 s), with the same colour coding. For the magenta cases the peaking was assumed only within* $\rho = 0.15$*; in all other cases it was within* $\rho = 0.3$*.*

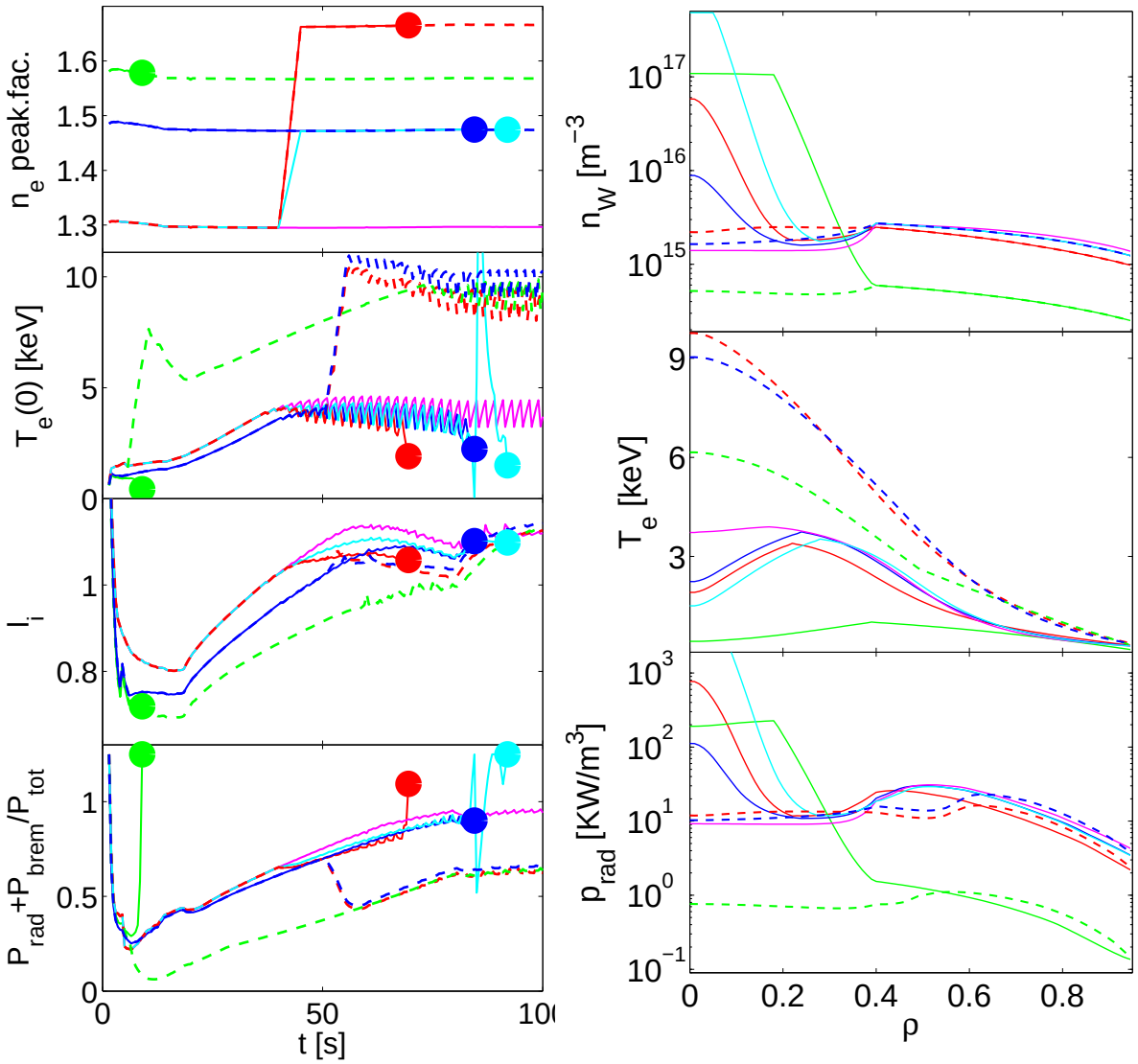

Figure 7. *Results of predictive modelling with* $n_{\rm W}$ *prescribed by Eqs.6,7. Shown are ohmic (full lines) and L-mode cases (dashed line). Left panel: time traces of* $n_{\rm e}$ *peaking,* $T_{\rm e}(0)$*,* $l_{\rm i}$ *and* $P_{\rm rad}$*. Right panel: profiles of* $n_{\rm W}$*,* $T_{\rm e}$ *and* $P_{\rm rad}$ *at the end of the* $I_{\rm p}$ *RU (80 s), or just before the simulated plasma is choked, with the same colour coding. Note the logarithmic scale for* $n_{\rm W}$ *and* $P_{\rm rad}$*.*

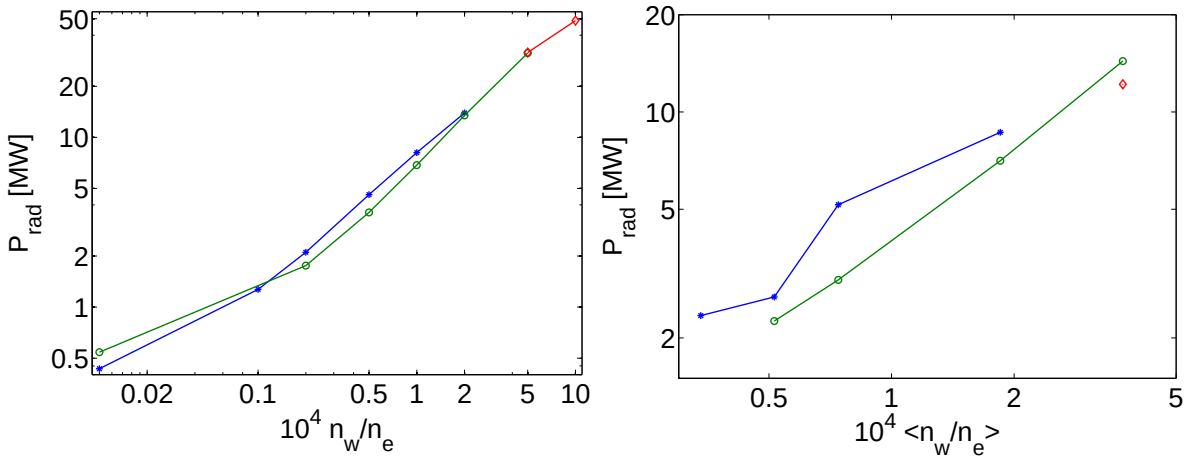

Figure 8. *$P_{\rm rad}$ as function of line averaged $n_{\rm W}(0)/n_{\rm e}(0)$ for the case of flat and peaked $n_{\rm W}/n_{\rm e}$ profiles (left, right, respectively) at 60 s, i.e. at 3/4 of the $I_{\rm p}$ RUfor ohmic (blue), L-mode with ECRH only (green), and L-mode with both ECRH and ICRF (red).*

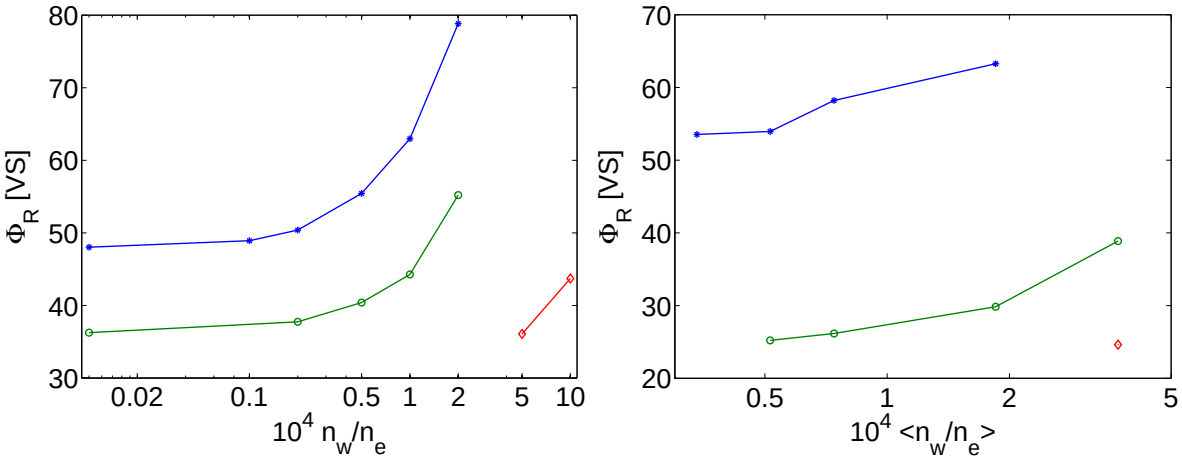

Figure 9. *Resistive flux consumption up to 60 s as function of line averaged* $n_{\mathrm{W}}(0)/n_{\mathrm{e}}(0)$ *for the case of flat and peaked* $n_{\mathrm{W}}/n_{\mathrm{e}}$ *profiles (left, right, respectively), for ohmic case (blue), for L-mode with 10/20 MW ECRH from 40 s (green), and for L-mode with 30-40 MW of additional power (ECRH plus ICRF) already from 10 s (red).*